Contents lists available at ScienceDirect

Biochimica et Biophysica Acta

journal homepage: www.elsevier.com/locate/bbabio

Review

Ultrafast infrared spectroscopy in photosynthesis ☆

Mariangela Di Donato [a,b,c], Marie Louise Groot [d,*]

[a] LENS (European laboratory for non linear spectroscopy), via N. Carrara 1, 50019 Sesto Fiorentino, FI, Italy
[b] Dipartimento di Chimica 'Ugo Schiff', Universita' di Firenze, via della Lastruccia 13, 50019 Sesto Fiorentino, FI, Italy
[c] INO (Istituto Nazionale di Ottica), Largo Fermi 6, 50125 Firenze, Italy
[d] VU University Amsterdam, Department of Sciences-Physics, LaserLab Amsterdam, De Boelelaan 1081, 1081 HV Amsterdam, The Netherlands

ARTICLE INFO

ABSTRACT

In recent years visible pump/mid-infrared (IR) probe spectroscopy has established itself as a key technology to unravel structure–function relationships underlying the photo-dynamics of complex molecular systems. In this contribution we review the most important applications of mid-infrared absorption difference spectroscopy with sub-picosecond time-resolution to photosynthetic complexes. Considering several examples, such as energy transfer in photosynthetic antennas and electron transfer in reaction centers and even more intact structures, we show that the acquisition of ultrafast time resolved mid-IR spectra has led to new insights into the photo-dynamics of the considered systems and allows establishing a direct link between dynamics and structure, further strengthened by the possibility of investigating the protein response signal to the energy or electron transfer processes. This article is part of a Special Issue entitled: Vibrational spectroscopies and bioenergetic systems.

© 2014 Elsevier B.V. All rights reserved.

1. Introduction

The key constituents of the photosynthetic apparatus of higher plants, algae and photosynthetic bacteria are pigment–protein complexes. The pigments harvest solar light via their electronic transitions that lie in a wide range of the solar spectrum and use that to drive a sequence of energy transfer and charge separation events, ultimately leading to a highly efficient transformation and storage of solar energy into chemical energy [1,2]. The elucidation of the kinetic and mechanistic aspects of the elementary steps involved in photosynthesis has significantly advanced since the realization of ultrafast techniques based on the employment of infrared (IR) laser pulses, enabling the recording of transient changes in vibrational transitions in real time. The vibrational spectrum of a protein or a protein-bound chromophore contains a wealth of information about the structure, the interaction with the environment and the electronic properties of the molecule, making the application of time-resolved spectroscopy in this spectral range particularly suited to elucidate the structure–function relationships determining the high efficiency of photosynthesis. This aspect is nowadays particularly important, as a good understanding of photosynthesis could provide precise guidelines for the realization of efficient solar cells with mechanistic and productive principles inspired by nature.

Starting with the pioneering work of Hochstrasser and coworkers [3], which in 1993 published the first report of a time-resolved study of the bacterial reaction center (RC) in the mid-IR (1800–1550 cm^{-1}), ultrafast pump–probe methods with sub-picosecond time resolution probing the infrared spectral range have developed as an important experimental tool. They have been applied to study energy and electron transfer in multiple systems, even in more intact photosynthetic systems such as the Photosystem II core or the Photosystem I antenna-RC complex [4–6].

The most informative spectral region for the study of photosynthetic systems is the 2500–1000 cm^{-1} range, where both the protein and the chlorophyll and carotenoid cofactors have their characteristic marker bands. The backbone protein is characterized by three fundamental IR bands: the amide I (mainly due to C=O stretching) at 1690–1620 cm^{-1}, the amide II (C–N stretching coupled with N–H bending) at ca 1550 cm^{-1} and the amide III (C–N stretching, N–H bending and C–C stretching) at ca 1300 cm^{-1}. Chlorophyll pigments are mainly probed through the absorption of their keto and ester C=O groups, which have significant absorption in the 1800–1650 cm^{-1} region, but other important modes can be identified in the lower frequency range, up to 900 cm^{-1}, due both to skeletal C–C and C–N stretching modes and to bending and combination ring modes [7,8]. As for carotenoids, the more informative region is around 1500 cm^{-1}, where C=C stretching modes are located [9,10].

One of the main advantages of infrared-based spectroscopies is the extreme sensitivity both to the conformation and to the particular environment in which a molecule is embedded. As an example, the exact

---

location at which a chlorophyll C=O group will absorb can vary by 30–40 cm^{-1} depending on the presence and number of H-bonds that the molecule can form and on the polarity of the environment [8]. Also, the oxidation state and the electronic state of the molecule, being the ground- or an excited-state, cause significant frequency shifts with respect to a reference situation [11]. This last aspect is particularly important in the study of photo-activated processes such as the energy and electron transfer events occurring in the photosynthetic systems, since the amount of shift of a particular vibration can give information on the electronic state or on the charge of the pigment to which it pertains. The application of a time-resolved method based on the use of visible-pump pulses, to trigger the photochemistry, and infrared-probe pulses, to follow the evolution of the vibrational response of the photoactivated system in time, has thus the advantage of being much more diagnostic for specific changes occurring at the molecular level than conventional visible pump/probe spectroscopy and, furthermore, opens the unique possibility to investigate the protein response to the light induced energy and electron transfer events.

Recording a high-resolution ultrafast infrared spectrum presents however several difficulties. A first problem is that the vibrational extinction coefficients are notably much lower than those of the electronic transitions, in a way that even the signals of the strongly absorbing chlorophyll C=O modes are usually about 200 times less intense than those of a typical chlorophyll electronic S$_0$ → S$_1$ absorption. The intensity of transient ΔAbs signals is therefore typically on the order of 0.1–0.4 mOD, which demands longer averaging times than in a visible pump–probe measurement in order to obtain good signal-to-noise ratio. Furthermore, the increased amount of structural information which can be retrieved in the IR has a price to pay, being the fact that the recorded spectra are highly congested and often difficult to interpret, due to the high number of vibrations pertaining to all the pigments involved in the photo-process that appear in the time resolved spectra. However the recourse to isotope labeling, the possibility of expressing site-specific mutants of the protein under study and the continuous progress of theoretical methods based on quantum chemical computations and molecular dynamic simulations, in combination with the availability of high resolution X-ray structure for the photosynthetic systems [12–14] can significantly help in the assignment of the vibrational bands to specific pigments.

Visible-pump/mid-IR-probe spectroscopy has been successfully applied in recent years to study multiple events occurring in different photosystems [4–6,15–20]. In this article we will review the most important results obtained in this field.

The paper is organized as follows: first we will present the basic principles of the technique and discuss the specific care to be taken in the acquisition and analysis of the time-resolved spectra of large protein–pigment complexes such as the photosynthetic systems. In the following sections we will review the most significant results obtained with these methods, discussing in different sections questions concerning charge separation, energy transfer, and the analysis of more intact systems, such as PSII-core and the PSI antenna-RC complex.

2. Methods

The application of the visible pump/mid-IR probe method to study photosynthetic systems started in 1993, when Hochstrasser and co-workers published a study on bacterial reaction centers in the region from 1800 to 1550 cm^{-1} with a time resolution of 60 ps [3]. They measured single wavelength traces using a tunable CW CO laser as probe, which was upconverted by a short 800-nm laser pulse in a non-linear crystal, and detected the intensity changes with a photomultiplier. Subsequently, using the same technique they improved the time resolution to 0.3–0.4 ps [21,22]. In 1995, the group of Zinth employed an array of 10 infrared detectors after dispersion of the IR-probe pulse in a grating spectrometer, monitoring the full bandwidth of the IR probe pulses (65 cm^{-1}) directly after each laser shot [23]. With the further

development of titanium sapphire lasers into all-solid state compact laser systems and the application of non-linear methods to generate the mid-infrared probe pulses, transient visible pump/mid-IR probe spectroscopy has now reached sub-picosecond time resolution and is widely applied to study a variety of photoinduced processes in proteins and particularly in photosynthesis.

In a typical setup for visible pump/midIR probe spectroscopy, infrared pulses tunable in the 3500–800 cm^{-1} range are obtained through difference frequency mixing (DFG) in an appropriate non-linear crystal (e.g. AgGaS$_2$) of two near-IR pulses of appropriate frequency (1200–2400 nm). The latter near-IR pulses are obtained through a white light-seeded optical parametric amplifier (OPA) configuration using a different non-linear crystal, usually BBO (β-BaB$_2$O$_4$) [24]. The output of such a OPA/DFG combination is typically a few microjoules when pumping with several hundred microjoules of the 800 nm fundamental of the amplified Ti:Sapph laser. The spectral width of the mid-IR pulse is determined by the bandwidth of the 800-nm pulse and the phase matching conditions of the crystal, typical values are a usable spectral width in the mid-IR of about 200 cm^{-1} for an 800 nm pulse of 85 fs. The pump pulses in the visible are in most cases obtained by pumping, with another portion of the 800-nm laser fundamental light, a non-collinear optical parametric amplifier [25–28] able to produce excitation pulses with a center wavelength tunable between 470 and 900 nm. The polarization of the excitation pulse with respect to the IR probe pulses is set with a Berek polarizer. The intensity of the visible pulses is attenuated to a value which depends on the experiment performed, typically 100 nJ or less. For a typical photosynthetic antenna sample, containing more than 10 chlorophylls, these pump energy conditions can induce multiple excitations in one complex and consequent annihilation processes. Experiments as a function of excitation density indicated that in the CP47 antenna complex, which contains 14 pigments connected by fast energy transfer, an excitation energy of 40 nJ/(150 μm)^2 is very close to annihilation free conditions [16]. For each experiment a careful choice of the operating conditions has to be performed, balancing the drop in the signal-to-noise ratio if low excitation densities are used against the annihilation processes that will occur as a result of multiple excitations in a multi-pigment complex when higher excitation densities are used. As experiments in the visible spectral region are easier to perform, it is often useful to calibrate the used power in the midIR experiment against a full excitation-density dependent study in the visible, to determine the amount of excitation annihilation that occurs and the effect it has on the time constants in the midIR experiment [15,16].

Both the vis-pump and mid-IR-probe pulses are then focused and spatially overlapped in the sample. In most cases the focusing lens of the mid-IR pulse is chosen to be stronger than that of the visible pulse to better match the size of the foci, which vary approximately with ~f × λ. After an overlap in the sample, the mid-IR probe pulses are dispersed in a spectrograph and imaged onto multiple-element MCT detectors. Commonly used MCT detectors consist of single or double (for reference purposes, see below) arrays of 32, 64 or 128 elements. Depending on the gratings used for the spectrograph and on the particular spectral region investigated, a spectral resolution of 2–6 cm^{-1} is achieved [29–33]. The signals of the detector array are then individually amplified, fed into integrate-and-hold devices, which are usually home-made in the various laboratories, and are read out on commercial acquisition cards after every shot. Alternatively, the mid-IR pulses can be detected by upconversion into the visible region where sensitive, cheaper detectors can be used with many more elements, such as a CCD line camera. A major breakthrough of this method was realized by the use of a chirped fundamental pulse [34] in a thin Mg doped LiNbO$_3$ crystal, with which a high spectral resolution of ~1 cm^{-1} could be realized, limited only by the later stages of the experimental setup. This method was subsequently applied to pump probe experiments [35,36] and multidimensional mid-IR spectroscopy [37,38]. A very broad IR window covering almost 600 cm^{-1} was realized with a resolution of 1 cm^{-1} [39], and the available spectral region

was extended to below 1800 cm^{-1}, i.e. between 900 and 2100 cm^{-1}, by using a AgGaGeS$_4$ optical crystal [40].

A phase-locked chopper operating at 500 Hz is used to ensure that every other shot the sample is excited, and/or a reference beam is used to probe an unpumped part of the sample, and the change in transmission and hence optical density between two consecutive shots can be measured. As in all pump–probe experiments the time-of-arrival difference between the pump and probe pulses is set by sending one of the two beams (generally the pump pulse) over a movable delay line. In case a second detector array is employed, the spectrum of a reference beam can be measured simultaneously and a ΔOD spectrum can be determined in a single shot, which can significantly reduce noise due to laser fluctuations. In general the stability of the experiment is determined by the noise in the probe pulse, which depends critically on the noise and dispersion of the 800 nm pulse, the alignment of the OPG/OPA, and on the time delay between the signal and idler pulse in the difference frequency generator [41]. After careful alignment, usually in 1 min of data collection the typical noise level of one single spectrum is 10^{-5} OD, implying a noise level of 30 μOD for a full data set consisting of 80 time points in a few hours [42]. Further sources of noise can be ascribed to the sample, which is usually placed in a movable scanner (see below), and can contain bubbles or small heterogeneities or be strongly absorbing.

To obtain overlap of visible and mid-IR pulses in time and space a thin slab of GaAs (50 μm thickness) can be used. The visible excitation pulse creates free electron carriers in this sample and thus a change in the index of refraction that results in huge changes in the transmission of the IR pulse, corresponding to several hundreds of mOD of absorption change. The cross correlation of the visible and IR pulses as measured in GaAs is typically about 180 fs. In a single experiment a spectral probe window of about 180 cm^{-1} (when a spectral resolution of 6 cm^{-1} is sufficient) is covered, so partly overlapping spectral regions must be measured to obtain a wider window. The excitation laser gives rise to a thermal lens effect in the sample, leading (due to its relatively long life time) to an offset in the channels when measuring the unpumped spectra. This effect is small and varies depending on the alignment between 0.1 and 1 mOD. However, compared to the small transient pump–probe signals this is still relatively large, but it can in general be corrected for by subtracting the signal before −10 ps. Perturbation by the pump pulse of the free induction decay signals of vibrational oscillators resulting from interaction with the probe pulse leads to signals observed in the time-window between ~−2 ps and 0 ps, as described by [43,44].

In order to extract the kinetic and spectral information from the time resolved spectra, great advantage comes from the application of global analysis methods [45–47], which are generally more suited to treat data where part of the noise is correlated (i.e. baseline noise or amplitude noise of the whole spectrum), and signals of different origin are strongly overlapping, as compared to a single-trace analysis. If the data contains sufficient information, or extra information is available from different kind of experiments, a target analysis can applied (i.e. a physical model is fitted to the data) from which the spectra of physical states and the intrinsic rates connecting them result.

2.1. Samples

Photosynthetic systems in general have a photocycle time longer than 1 ms. Therefore, to ensure a fresh sample spot for each laser shot and reduce photodegradation, usually the samples are placed into movable scanners. Particularly suited for this purpose are Lissajous sample scanners, where the sample is moved perpendicular to the beam on three eccentrics, and, depending on the velocity of the scanner, the laser comes back at the same sample position on a minute timescale [42]. If an excitation spot size of 150 μm and a repetition rate of 1 kHz are used, the sample must be moved at a speed of 0.15 m/s. This refreshment speed can be obtained in the Lissajous scanner, but not at the corners where the

scanner changes direction. The data collected at these points (15–18% of the total number of acquisitions) have to be excluded from the result. Alternatively a flow cell can be used, requiring however higher sample amounts, which can often be a problem with the high sample concentrations necessary to perform mid-IR experiments. Another way to reduce photodegradation and photoaccumulation of radical/charged species in the sample is to reduce the laser repetition rate below the generally employed 500 Hz value. Too low refreshment rates can be recognized by a negative pump–probe-like signal before t = 0 when a pump-reference pulse sequence is collected with subsequent laser shots, as the reference (partially) probes the photoproduct induced by the pump pulse.

The samples are usually contained in demountable cells consisting of 2 CaF$_2$ plates separated by a Teflon spacer of variable thickness (usually 10–50 μm).

Photosynthetic samples are prepared at very high concentrations to reduce the amount of water, which strongly absorbs in the mid-IR range and would otherwise greatly absorb the probe beam. Although very concentrated, the analyzed systems are still generally in a liquid buffer solution phase, and not completely dried, in order to obtain the most homogeneous sample possible. Often the buffer solution is prepared in D$_2$O, in order to minimize water absorption in the amide region. Typically, the photosynthetic protein samples are prepared such that they have an OD$_{max}$ in the visible (Q$_Y$ region) between 0.2 and 0.5 per 20 micrometer path length, to ensure homogeneous excitation over the sample. They have then a similar absorption around 1650 cm^{-1}. When necessary, depending on the composition of the sample and which photoinduced process has to be studied, redox mediators can be added to the sample solution, such as sodium ascorbate and/or phenazine methosulfate (PMS) to prevent photoaccumulation of RCs in the P$^+$ state, as described in [19].

3. Charge separation

3.1. Bacterial reaction center

Charge separation in bacterial reaction centers has been the subject of the earliest vis-pump mid-IR probe studies with sub-ps time resolution. This pigment–protein complex contains 4 bacteriochlorophylls and two bacteriopheophytins arranged symmetrically along two branches, denoted as A and B. Light absorption by the 'special pair' P, a bacteriochlorophyll dimer, initiates charge separation along the A branch, leading to the stabilization of a negative charge on the bacteriopheophytin H$_A$ in 3–4 ps, and subsequently on the primary quinone acceptor Q$_A$ in 200 ps, for reviews see [1,2,48,49]. Early midIR studies were able to observe the formation of the charge separated state P$^+$H$_A^-$ in 3 ps, as well as the bands ascribed to the electronic states corresponding to a P* inter-exciton transition and those of the P$^+$ electron hole transition between the two halves of the dimer, located at around 2400 cm^{-1} [21,22]. The stabilization of a positive charge on P was recognized by the appearance of a characteristic double peaked structure at 1714 and 1704 cm^{-1}, due to the keto of P$_L^+$ and P$_M^+$ respectively [50–52], which are at ~1680 cm^{-1} in the P ground state, while the localization of the negative charge on H$_A$ was signaled by the absorption of its keto mode at 1591 cm^{-1} and the corresponding ground state bleaching at 1675 cm^{-1} [53,54]. After these initial investigations, time resolved studies probing the 1600–1800 cm^{-1} spectral region were repeated with improved time- and spectral-resolution, focusing on the identification of characteristic spectral signature of the monomer chlorophyll B$_A$, located between the special pair P and the bacteriopheophytin, in order to confirm its participation to the charge separation process see Fig. 1 [18,55]. The formation of the charge separated state P$^+$B$_A^-$ was followed both upon direct excitation of P at 860 nm and upon B$_A$ excitation at 800 nm. The B$_A^-$ anion was characterized by a 9-keto bleaching signal, located at 1670–1680 cm^{-1}, which appeared in the time resolved spectra 3.7 ps after excitation. The characteristic signatures of the charge separated state
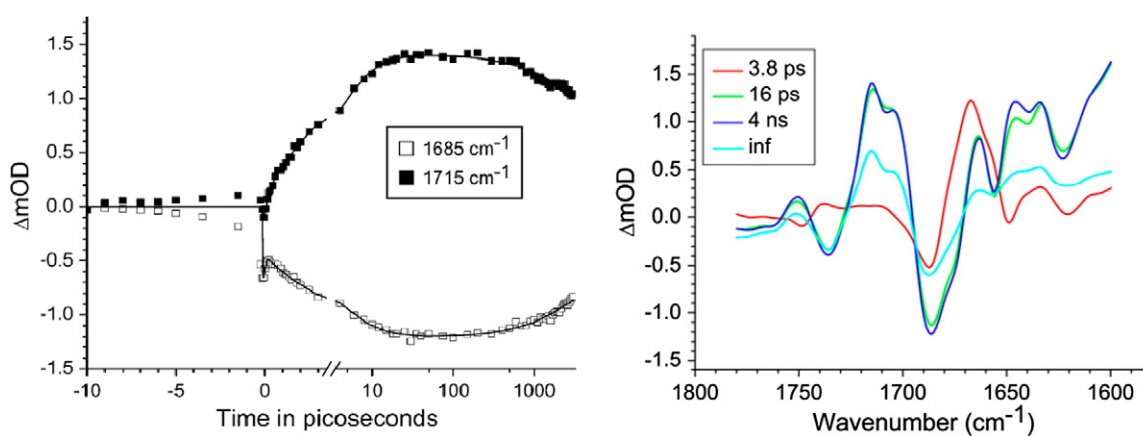
Fig. 1. Sub-picosecond visible pump/midIR probe experiments on R26 RCs lacking Q_A. Time-traces collected at two characteristic frequencies (symbols) and fit resulting from a global analysis of 32 time traces (solid lines, left panel). Evolution-associated difference-spectra (EADS) resulting from a global analysis using a sequential model with increasing lifetimes. The measurements were carried out over a 1780–1600 cm^{-1} window with a spectral resolution of 6 cm^{-1}. Reproduced from [18].

$P^+H^-_A$ appeared 1 ps after the localization of the negative charge on B_A. As the mid-IR difference spectra of $P^+B^-_A$ and $P^+H^-_A$ strongly resembled each other, the mid-IR data could add little to the body of knowledge on the cofactors and time scales involved in charge separation collected via vis- and near-IR spectroscopy, for reviews on this topic see [1,2,48,49]. However, the analysis of the mid-IR data did reveal a protein response to the photoinduced processes and small changes in the localization of the hole on the P dimer constituents. The relaxation of the charge separated state $P^+H^-_A$ on a 20 ps time scale was observed to be accompanied by a change in the relative ratio of the P_A and P_B bands and by a minor change in the amplitude of a band at 1640 cm^{-1} ascribed to the response of an amide C=O to the radical pair formation. The relaxation of the charge separated state $P^+H^-_A$ is caused by a lowering of the free energy, the observation of a change in P_A and P_B band intensity on the same time scale strongly suggests that the drop in free energy is associated with an increased localization of the electron hole on the P_A half of the dimer [18].

3.2. D1D2 reaction center of plant Photosystem II

The D1D2 reaction center is the minimal unit of plant Photosystem II still able to perform a light-driven charge separation. D1D2 is structurally similar to the bacterial RC, containing 4 chlorophylls and 2 pheophytins, arranged along two symmetric branches, denoted as D1 and D2. Like in the bacterial RC, light-induced electron transfer occurs only along one of the two branches. Besides those pigments, D1D2 also contains two additional chlorophylls bound to the periphery of the complex, which transfer excitation energy slowly into the core. All these pigments have their lowest energy absorption band near 675 nm, in contrast to the bacterial RC, where each (type of) pigment is characterized by a well-separated absorption band in the near-IR. Another contrast with the bacterial RC is that in the PSII RC the initial dynamics are highly multi-exponential with lifetimes in the order of 100 and 300–400 fs, and 3, 10, and 30 ps [56–65]. These dynamics all represent a mixture of energy transfer, excited state decay, radical pair-formation and relaxation, in part due to the shallow equilibria between the excited pigments and the initial radical pair state(s). In the visible part of the spectrum, radical pair states have to be differentiated from excited states by an absence of stimulated emission, which itself is difficult to distinguish from bleached absorption, because of the very small Stokes shift in these chlorophylls [66]. A recourse to extending the probed spectral region to the near-UV or to 2D electronic spectroscopy did not result in the observation of more defining features for specific pigments or radical pair states [66, 67]. These problems have for a long time resulted in difficulty in identifying the intrinsic charge separation rate and in identifying the primary electron donor [56–65]. Several groups suggested that not P680, the equivalent of the P-dimer in the BRC, is the primary electron donor, but the 'accessory' Chl on the D1 branch and that electron transfer starts with the formation of the pair $Chl^+_{D1}H^-_{D1}$: (i), in analogy with the alternative electron transfer pathways in bacterial RCs [68–70]; (ii), on the basis of its proposed red absorption [71]; (iii), its proposed oxidation potential [72]; (iv), the strong pheophytin Stark signal interpreted as a charge transfer state $Chl^{\delta+}_{D1}H^{\delta-}_{D1}$ [73]; and (v) the analysis of photon echo data [74]. Also, 77 K vis pump-vis probe data recorded at 77 K [66] were analyzed with a model in which charge separation occurs from both the accessory chlorophyll and from the special pair [75].

In the mid-IR, the formation of chlorophyll cation and anion states gives rise to well-defined bands in the vibrational spectrum [76–81]. The evolution of these bands gives information of the involvement of subsequent electron donors and acceptors. Following excitation at 669 nm or 680 nm, mid-IR difference spectra recorded between 100 fs and 3 ns revealed the presence of several different keto groups whose relative population changed in response to energy and electron transfer, as shown in Fig. 2 [17]. Immediately after photoexcitation the keto modes of the excited chlorophylls downshifted from the 1700 cm^{-1} to the 1660 cm^{-1} region, giving rise to a broad absorption band. In the following, as charge separation occurs, dynamics in the region specific for the Chl cation and pheophytin anion states, as identified in steady state FTIR spectroscopy [76–81] could be observed. The long-lived (>ns) difference spectrum showed a very good agreement with steady-state P^+H^- spectra, with P^+/P positive peaks at 1724 and 1713 cm^{-1} and a negative peak at 1702 cm^{-1}, and H^-/H negative peaks at 1739, 1722 and 1677 cm^{-1}, and a positive peak at 1731 cm^{-1}. To extract information on the dynamics leading up to this state a target analysis had to be applied, with, since the energy and electron transfer processes are reversible, a model taking into account the equilibria between the different states, as depicted in Fig. 2. This target analysis yielded a spectrum of a radical pair formed prior to the final P^+H^- state, which contained clear H^-/H features, but in which those of P^+/P were notably absent and instead contained cation features of another Chl molecule. This observation led to the conclusion that in D1D2 the initial electron donor is not the special pair P, but the monomer chlorophyll Chl_{D1}, located on the D1 branch between P and H_{D1}. The formation of the Chl^+_{D1}/H^- radical pair occurred within 1 ps, and P^+ was only formed on a timescale of a few ps, by successive electron transfer to Chl^+_{D1} [17].

4. Energy transfer

Even more than in the case of charge separation in D1D2 reaction centers, the analysis of time-resolved spectra in the IR applied to
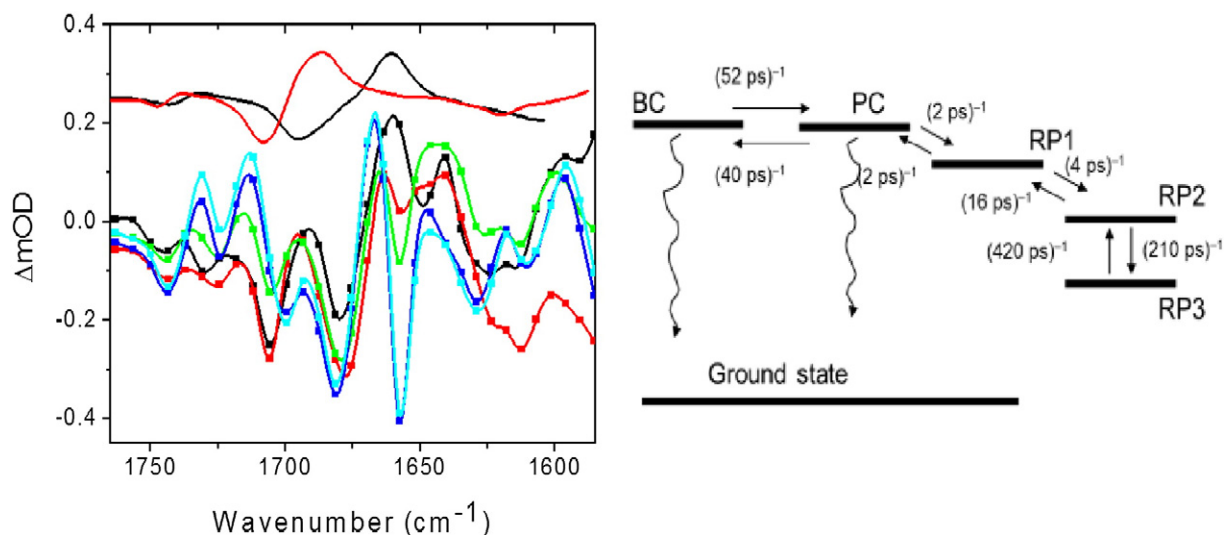
Fig. 2. Sub-picosecond visible pump/midIR probe experiments on D1D2 reaction centers of Photosystem II using excitation at 669 nm. Evolution associated difference spectra resulting from a global analysis using a sequential model with increasing lifetimes (right). The Chl*/Chl (black line) and H*/H (red line) excited state difference spectra in THF measured 10 ps after excitation at 530 nm are shown (upper curves, right panel) for comparison. Lifetimes are 0.2 ps (black), 3 ps (red), 32 ps (green), 2 ns (blue) and infinite (cyan). Kinetic target model (left) applied to extract information on the energy and electron transfer processes from the data. BC and PC: excited states; RP1: radical pair $Chl_{D1}^+H_{D1}^-$; RP2: radical pair $P^+H_{D1}^-$; RP3: radical pair $P^+H_{D1}^-$ relaxed. A smooth line has been drawn through the measuring points as a guide for the eye. Reproduced from [17].

study energy transfer in antenna systems has a notable advantage over time-resolved studies in the visible spectral range. Also in antenna systems the absorption of the multiple pigments linked to light-harvesting protein results in a single visible band, centered at 675 nm in the case of chlorophyll a or 650 nm for chlorophyll b, which makes a detailed connection between the structure and the role of the different pigments in the flow of energy through the complex very difficult. The availability of high resolution crystal structures of the core of Photosystem II [82–84] containing the two peripheral antenna complexes CP43 and CP47 and the main antenna LHCII [85] allows in principle to assign a spectral signature in the IR to specific chlorophylls, based on the expected location of their keto and ester frequencies as a function of the local environment. On these premises the dynamics of energy transfer in both the peripheral PSII core antennas CP43 and CP47 and in the major antenna LHCII have been studied with transient absorption methods in the infrared spectral range [15,16,20]. In order to correlate the population of blue and red-absorbing pigments in the visible spectrum with the population of Chls with keto modes at different frequencies, simultaneous measurements of the visible absorption changes with those in the mid-IR, as a function of excitation density were carried out.

4.1. CP43–CP47

CP43 and CP47 are small antenna proteins present in the Photosystem II core of higher plants. CP43 binds 14 chlorophyll a molecules and 3 β-carotenes (Car), CP47 17 Chls a and 4 β-Cars. Visible pump–probe absorption difference spectra typically reveal only very limited spectral evolution to occur in these complexes [15,16,86,87], as is illustrated Fig. 3. The absorption changes in the mid-IR upon excitation of CP47 and CP43 at 590 nm on the other hand, reveal a set of different keto frequencies in each spectrum of which the relative population changes as energy transfer and annihilation processes take place [15,16] (see Fig. 3). In both complexes the bleached ground state keto bands at 1700–1660 cm^{-1} are fairly well separated from the keto modes in the excited state in the region 1660–1600 cm^{-1}, and a careful analysis of the evolution of these signatures, in combination with structural information, can reveal precise details on the flow of energy through the complexes. In the case of CP43, for instance, energy transfer was found to occur on time scales of 250 fs, 2–4 ps and 10–12 ps. The vis/mid-IR difference spectra showed that the excitation is initially distributed over chlorophylls located in environments with different
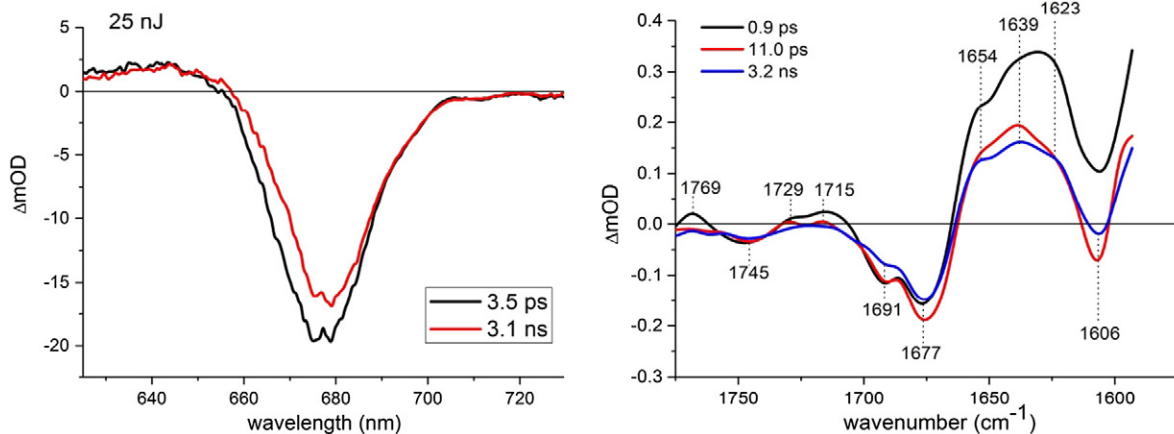

Fig. 3. Evolution associated difference spectra (EADS) obtained by global analysis of the transient absorption data measured on CP43 upon 590 nm excitation, probing the visible region (left panel) and the mid-IR region (right panel). A sequential kinetic scheme with increasing lifetimes was used. In the mid-IR several bleaching bands can be distinguished, due to the absorption of carbonyl and ester residues pertaining to chlorophyll molecules located in different polar environments. For more details, see [15].

polarities, since two 9-keto C=O stretching bleachings, at 1691 and 1677 cm^{-1}, are observable at early delay times [15]. Furthermore, positive signals in the initial difference spectra around 1750 and 1720 cm^{-1} indicated the presence of a charge transfer state between strongly interacting chlorophylls, which is hardly recognized in the visible spectra. The combined study of infrared and visible data, recorded at different excitation energies in order to increase the amount of annihilation processes in the systems to enhance spectral dynamics, led to conclusion that there are in the complex two fairly isolated red absorbing pigments, not connected with the bulk chlorophylls on a 10 ps time scale. Based on the exact location of the infrared modes observed in the transient spectra it was concluded that at least some of these red absorbing pigments are located in a polar environment, possibly forming H-bonds with the surrounding protein. Very similar conclusions were drawn for the CP47 antenna [16]: two red (683-nm) pools, plus an additional red-shifted one (690 nm) were found to have a keto C=O stretching frequency at 1686 cm^{-1} and therefore concluded to be in a polar environment or have a fairly weak hydrogen bond. For the more blue-absorbing states, varying keto band positions between 1696 and 1664 cm^{-1} were observed, and thus their hydrogen bond strengths varied between "none present" and "strong". A change in the frequency of the coordination marker mode was observed when the 690-nm state was populated, probably caused by a more planar conformation of the macrocycle of the chlorophyll responsible for the 690-nm state [16]. We would like to note here that the spectral dynamics in the visible datasets, collected as a function of excitation density, were assigned to annihilation [15, 16]. However, these data show a remarkable likeness to data later collected as a function of excitation density on aggregates of Pchlide in solution [88], that were successfully modeled with a refined multiexciton model that includes static disorder. It was found that population up to the 4-exciton manifold was sufficient to explain the pronounced saturation of the bleaching and the shape changes in the instantaneous, t = 0.2 ps spectra [89]. Furthermore, the exciton states in the Pchlide aggregates were suggested to be mixed with charge-transfer states (CTS), that could also explain the observation of excited state spectra with cation-like features in the CP43 mid-IR difference spectra [15].

4.2. LHCII

The trimeric light harvesting complex II (LHCII) is the most abundant protein in the thylakoid membrane of higher green plants and green algae. The high resolution crystal structure of this system has been resolved, showing that in the native trimeric system each monomer contains 6 chlorophyll b, 8 chlorophyll a molecules and four carotenoids.[85] A variety of studies, performed to analyze the dynamics of excitation energy transfer within the LHCII complex, suggest that Chl b to Chl a transfer and transfer among Chl a pigments occur with time constants of 150–300, 600 fs, 2–5 ps and 10–20 ps [90–100]. Additional information, as obtained from the application of theoretical modeling based on a modified Redfield relaxation theory [101,102] led to a picture in which dimers or trimers of very closely lying pigments equilibrate on a very fast sub-picosecond timescale, followed by energy transfer between clusters on the stromal and luminal sides. The isolated position of a Chl b (b605 in the Liu nomenclature [85]) and a Chl a (a604) molecule in the structure leads to a very slow transfer from and to these pigments, the so-called "bottleneck states" [102]. The analysis of time resolved studies in the IR, applied to the LHCII complex, confirmed all the information on the timescale of the energy flow within the system as suggested from previous studies [20]. However, additional information on the location of the bottleneck pigments could be retrieved with this technique. A careful analysis of the evolution of the time-resolved spectra in the IR, in connection with structural information from the available crystal structure allowed for proposing the assignment of the IR bands observed in the spectra to specific pigments. In particular, it was found that a keto band at 1680 cm^{-1} was populated only on a slow 6–8 ps time scale, and depopulated on a slow 30–40 ps

timescale. This band was thus assigned to the bottleneck state, located on Chla604. The downshifted position of this keto mode absorption, indicating the presence of an H-bond, is compatible with structural information from the crystal structure, showing that Chl a604 can indeed participate in a hydrogen bond, since it is at a short distance from Leu 113N [85].

5. Photosynthetic core-systems

5.1. PSII-core

Experiments have also been performed on the larger core particles of PSII, containing the CP43 and CP47 antenna proteins and the D1D2 RC with a total of 36 chlorophylls and 2 pheophytin pigments [4,6]. Of course, upon light absorption most of the excitations will be localized on the two core antenna complexes, CP43 and CP47, implying that the observed kinetics of charge separation will be limited by the amount of time it takes to transfer excitations from CP43/CP47 to the RC. For this reason data interpretation required the recourse to a kinetic model including both energy transfer pathways from the antennas and charge separation within the D1D2 RC. Based on this kinetic scheme, and with the previously acquired knowledge of the IR difference spectra for the constituents CP43, CP47 and the D1D2-RC that together form the PSII-core complex, it was possible to follow the features specific for each of the PSII core constituents in time. The presence of CP43 and CP47 specific features in the spectra up to time delays of 20–30 ps led to the conclusion that the main part of the energy transfer from the antenna's to the RC occurs on this time scale. Direct excitation of the pigments in the RC led to the radical pair formation of $P^+_{D1}H^-_{D1}$ on the same time scale as multi-excitation annihilation and excited state equilibration within the antennas CP43 and CP47, which occur within ~1–3 ps. The formation of the earlier radical pair $Chl^+_{D1}H^-_{D1}$, as identified in isolated D1D2 complexes with time-resolved mid-IR spectroscopy [103] was not resolved in cores probably due to its relatively low concentration [6]. However, later experiments on the PSII core complex from the cyanobacterium *Synechocystis* sp. PCC 6803 and comparison with two site directed mutants where the histidine residue directly coordinated to the P_B chlorophyll had been exchanged with alanine or glutamine, allowed for the identification of specific spectral signatures of the monomer chlorophyll B_A, confirming the participation of this residue in the charge separation process, as observed in isolated D1D2 RCs [4]. Finally, the experiments performed on intact core particles definitively showed that the time resolved IR-difference spectrum of $P^+_{D1}H^-_{D1}$ as observed in these large systems is virtually identical to that observed in the isolated D1D2-RC complex of PSII, demonstrating that the local structure of the primary reactants remains intact in the isolated D1D2 complex [4,6].

5.2. PSI-core

PSI is one of the largest membrane proteins for which a crystal structure has been resolved [104,105] and consists of 11–13 protein subunits, binding approximately 90–100 chlorophyll pigments. The two largest subunits, denoted as PsaA and PsaB, form a heterodimer, which binds most of the core antenna pigments as well as the cofactors of the reaction center (RC). As in Photosystem II, the reaction center's pigments are symmetrically distributed on the two PsaA and PsaB subunits, but, in this case, a growing number of experimental investigations suggest that the electron transfer reactions can occur along both branches of the RC [106–114,20]. Resolving the primary energy and electron transfer kinetics in PSI is very challenging, since in this system the reaction center cannot be isolated from the primary antenna, meaning that time-resolved experiments have to be performed on a system containing about 100 chlorophylls. In addition, the appearance of cation and anion Chl states in the 650–750 nm region is signified by the loss of stimulated emission only. This has led to uncertainty about the precise

identity of the primary electron donor and acceptor pair in PSI [115, 116].

Even in this large system it proved possible to study the dynamics of energy and electron transfer with femtosecond vis-pump/mid-infrared-probe spectroscopy [5]. In order to highlight the different contributions coming from the antennas or RC chlorophylls, and in particular to isolate signals of the red chlorophylls, three different excitation wavelengths were used, 700, 710 and 715 nm. Chlorophyll cation signals were observed to rise faster than the time resolution of the experiment (~0.2 ps) upon both excitation conditions; 700 nm and selective red excitation. A further rise of the cation signals on a sub-picosecond time scale (0.8–1 ps) indicated the formation of the primary radical pair. Evolution in the cation region with time constants of 7 ps and 40 ps revealed the formation of the secondary radical pair, involving a different set of electron donor and acceptor molecules. The IR signatures of the second RP agreed well with the FTIR difference spectra previously reported for the $P_{700}^{+}A_{1}^{-}$ state [107,117–120], see Fig. 5. As the pairs of chlorophyll molecules denoted as A and A_0 are located in between P700 and the phylloquinone A_1, it was proposed that A and A_0 constitute the primary radical pair [5]. To disentangle the spectra of the involved radical pairs from the data and determine the intrinsic electron transfer rates, two target models were used that differed in assigning the cationic features observed at t = 0 to either ultrafast charge separation or to the red pigments in PSI having a charge transfer character, see Fig. 4. In both models, the intrinsic initial charge separation forming $A^{+}A_{0}^{-}$ was very fast, 3 ps^{-1}. In addition, the secondary electron transfer step, leading to reduction of the quinone cofactor A_1, was faster than previously reported: the models consistently showed that in about 6 ps an equilibrium between $A^{+}A_{0}^{-}$ and $P_{700}^{+}A_{1}^{-}$ was formed. After 40 ps, this equilibrium shifts towards a full population of $P_{700}^{+}A_{1}^{-}$. The 40 ps time constant was in good agreement with literature reports [107]. However, the intrinsic rate of reduction of A_1 was now resolved to be $(6\ ps)^{-1}$, due to the high specificity of the A_{1}^{-}/A_{1} signals in the mid-IR. This makes the reduction of the quinone in PSI not one, but two orders of magnitude faster than that of H_{A}^{-} reoxidation by Q_A in type II RCs (see also [121]). Furthermore, a comparative measurement of open (where the secondary acceptor A_1 is not reduced) and closed (where the secondary acceptor A_1 is already reduced) PSI cores showed that even closed systems are able to perform the first step of charge separation [122].
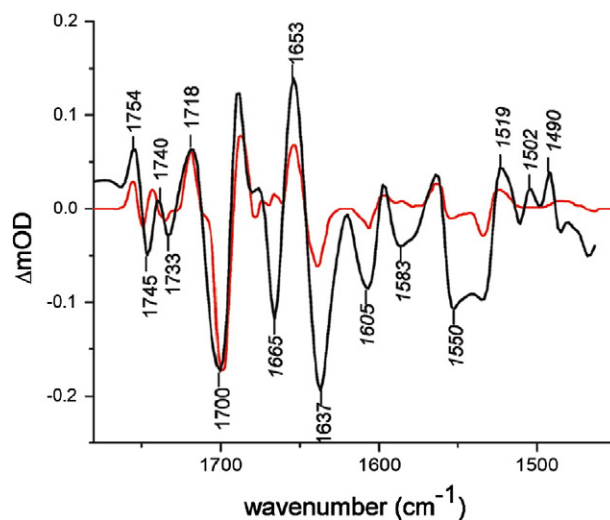

Fig. 5. Comparison between the FTIR spectrum of $P_{700}^{+}A_{1}^{-}$ (adapted from reference [107]) and the time-resolved second radical pair spectrum measured with vis pump mid-IR probe in PSI. Reproduced from [5].

6. Concluding remarks

The application of mid-infrared absorption difference spectroscopy with sub-picosecond time-resolution to photosynthetic complexes has been extremely fruitful. In each of the complexes that it has been applied to, it has led to new insights: either by identifying a primary radical pair state due to the clear signature in the mid-IR of chlorophyll cation and anion states, or by enabling the link between dynamics and structure to be made, or by demonstration of a protein response signal. The success of 'femtoIR' is in part due to the fact that it could build upon the body of knowledge on these photosynthetic systems created by steady-state FTIR spectroscopy. This enabled a qualitative comparison of spectra leading to the discussed insights in photosynthetic processes. However, a full quantitative understanding of the IR-difference spectra is lacking. In future, it would be a great asset to be able to accurately and reliably calculate IR-difference spectra with advanced quantum chemical modeling [123,124] and thus explore the full information
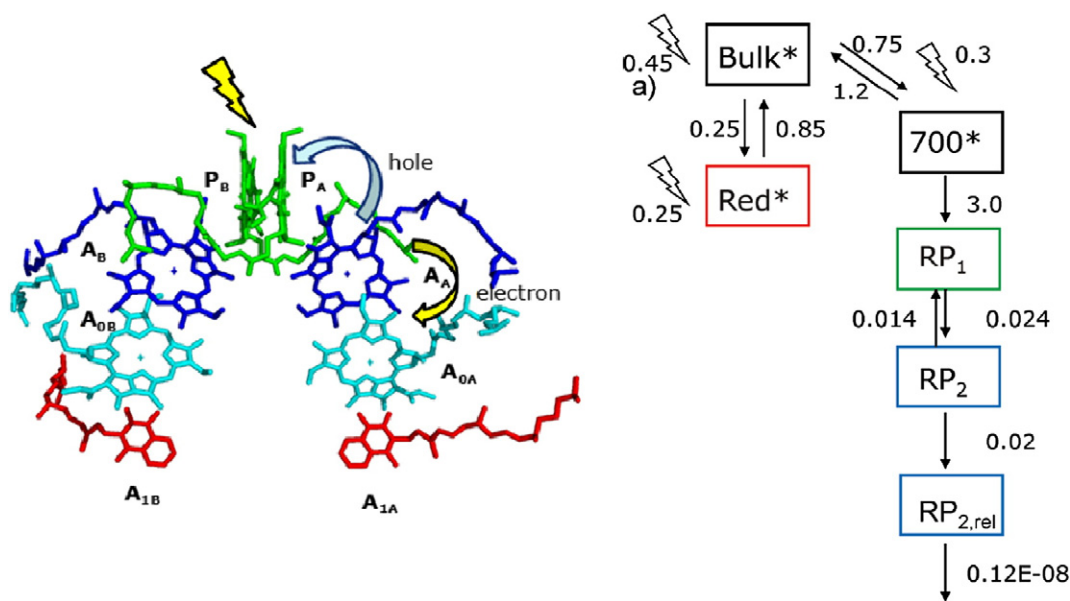

Fig. 4. Cofactor arrangement in the RC of PSI and kinetic scheme used for the target analysis of time resolved infrared data. Rates are given in ps^{-1}. RP1 and RP2 were assigned to the states $A_{A}^{+}A_{0A}^{-}$ and $P_{700}^{+}A_{1A}^{-}$, respectively, based on the retrieved difference spectra and their comparison with FTIR spectra. Reproduced from [5].

content of the IR spectra, retrieve details on the environment and structure of the molecule and so make full use of femtoIR spectroscopy as the link between structure and dynamics.

Acknowledgements

References

[1] J. Deisenhofer, J.R. Norris (Eds.), The Photosynthetic Reaction Center, Academic Press, New York, 1993.

[2] Molecular Mechanism of Photosynthesis, in: R.E. Blankenship (Ed.), Blackwell Science, Oxford, 2002.

[3] S. Maiti, B.R. Cowen, R. Diller, M. Iannone, C.C. Moser, P.L. Dutton, R.M. Hochstrasser, Picosecond infrared studies of the dynamics of the photosynthetic reaction center, Proc. Natl. Acad. Sci. U. S. A. 90 (11) (1993) 5247–5251.

[4] M. Di Donato, R.O. Cohen, B.A. Diner, J. Breton, R. van Grondelle, M.L. Groot, Primary charge separation in the photosystem II core from Synechocystis: a comparison of femtosecond visible/midinfrared pump–probe spectra of wild-type and two P_{680} mutants, Biophys. J. 94 (12) (2008) 4783–4795.

[5] M. Di Donato, A.D. Stahl, I.H.M. van Stokkum, R. van Grondelle, M.L. Groot, Cofactors involved in light-driven charge separation in photosystem I identified by subpicosecond infrared spectroscopy, Biochemistry 50 (4) (2011) 480–490.

[6] N.P. Pawlowicz, M.L. Groot, I.H.M. van Stokkum, J. Breton, R. van Grondelle, Charge separation and energy transfer in the photosystem II core complex studied by femtosecond midinfrared spectroscopy, Biophys. J. 93 (8) (2007) 2732–2742.

[7] M. Fujiwara, M. Tasumi, Resonance Raman and infrared studies on axial coordination to chlorophylls a and b in vitro, J. Phys. Chem. 90 (2) (1986) 250–255.

[8] J.J. Katz, G.L. Closs, F.C. Pennington, M.R. Thomas, H.H. Strain, Infrared spectra, molecular weights, and molecular association of chlorophylls a and b, methyl chlorophyllides, and pheophytins in various solvents, J. Am. Chem. Soc. 85 (23) (1963) 3801–3809.

[9] S. Saito, M. Tasumi, Normal-coordinate analysis of β-carotene isomers and assignments of the Raman and infrared bands, J. Raman Spectrosc. 14 (5) (1983) 310–321.

[10] Y. Koyama, I. Takatsuka, M. Nakata, M. Tasumi, Raman and infrared spectra of the all-trans, 7-cis, 9-cis, 13-cis and 15-cis isomers of β-carotene: key bands distinguishing stretched or terminal-bent configurations form central-bent configurations, J. Raman Spectrosc. 19 (1) (1988) 37–49.

[11] W.G. Mantele, A.M. Wollenweber, E. Nabedryk, J. Breton, Infrared spectro-electrochemistry of bacteriochlorophylls and bacteriopheophytins: implications for the binding of the pigments in the reaction center from photosynthetic bacteria, PNAS 85 (22) (1988) 8468–8472, http://dx.doi.org/10.1073/pnas.85.22.8468.

[12] A. Ben-Shem, F. Frolow, N. Nelson, Crystal structure of plant photosystem I, Nature 426 (6967) (2003) 630–635.

[13] N. Kamiya, J.R. Shen, Crystal structure of oxygen-evolving photosystem II from Thermosynechococcus vulcanus at 3.7-angstrom resolution, Proc. Natl. Acad. Sci. U. S. A. 100 (1) (2003) 98–103.

[14] Y. Umena, K. Kawakami, J.R. Shen, N. Kamiya, Crystal structure of oxygen-evolving photosystem II at a resolution of 1.9 angstrom, Nature 473 (7345) (2011) 55–U65.

[15] M. Di Donato, R. van Grondelle, I.H.M. van Stokkum, M.L. Groot, Excitation energy transfer in the photosystem II core antenna complex CP43 studied by femtosecond visible/visible and visible/mid-infrared pump probe spectroscopy, J. Phys. Chem. B 111 (25) (2007) 7345–7352.

[16] M.L. Groot, J. Breton, L. van Wilderen, J.P. Dekker, R. van Grondelle, Femtosecond visible/visible and visible/mid-IR pump–probe study of the photosystem II core antenna complex CP47, J. Phys. Chem. B 108 (23) (2004) 8001–8006.

[17] M.L. Groot, N.P. Pawlowicz, L. van Wilderen, J. Breton, I.H.M. van Stokkum, R. van Grondelle, Initial electron donor and acceptor in isolated Photosystem II reaction centers identified with femtosecond mid-IR spectroscopy, Proc. Natl. Acad. Sci. U. S. A. 102 (37) (2005) 13087–13092.

[18] N.P. Pawlowicz, R. Van Grondelle, I.H.M. van Stokkum, J. Breton, M.R. Jones, M.L. Groot, Identification of the first steps in charge separation in bacterial photosynthetic reaction centers of Rhodobacter sphaeroides by ultrafast mid-infrared spectroscopy: electron transfer and protein dynamics, Biophys. J. 95 (3) (2008) 1268–1284.

[19] A.D. Stahl, L.I. Crouch, M.R. Jones, I. Stokkum, R. Van Grondelle, M.L. Groot, Role of PufX in photochemical charge separation in the RC-LH1 complex from Rhodobacter sphaeroides: an ultrafast mid-IR pump–probe investigation, J. Phys. Chem. B 116 (1) (2012) 434–444.

[20] A.D. Stahl, M. Di Donato, I. van Stokkum, R. van Grondelle, M.L. Groot, A femtosecond visible/visible and visible/mid-infrared transient absorption study of the light harvesting complex II, Biophys. J. 97 (12) (2009) 3215–3223.

[21] S. Maiti, G.C. Walker, B.R. Cowen, R. Pippenger, C.C. Moser, P.L. Dutton, R.M. Hochstrasser, Femtosecond coherent transient infrared-spectroscopy of reaction centers from Rhodobacter sphaeroides, Proc. Natl. Acad. Sci. U. S. A. 91 (22) (1994) 10360–10364.

[22] G.C. Walker, S. Maiti, B.R. Cowen, C.C. Moser, P.L. Dutton, R.M. Hochstrasser, Time resolution of electronic-transitions of photosynthetic reaction centers in the infrared, J. Phys. Chem. 98 (22) (1994) 5778–5783.

[23] P. Hamm, M. Zurek, W. Mantele, M. Meyer, H. Scheer, W. Zinth, Femtosecond infrared-spectroscopy of reaction centers from Rhodobacter sphaeroides between 1000 and 1800 cm^{-1}, Proc. Natl. Acad. Sci. U. S. A. 92 (6) (1995) 1826–1830.

[24] R.A. Kaindl, M. Wurm, K. Reimann, P. Hamm, A.M. Weiner, M. Woerner, Generation, shaping, and characterization of intense femtosecond pulses tunable from 3 to 20 μm, J. Opt. Soc. Am. B Opt. Phys. 17 (12) (2000) 2086–2094.

[25] G. Cerullo, M. Nisoli, S. Stagira, S. De Silvestri, Sub-8-fs pulses from an ultrabroadband optical parametric amplifier in the visible, Opt. Lett. 23 (16) (1998) 1283–1285.

[26] A. Shirakawa, I. Sakane, T. Kobayashi, Pulse-front-matched optical parametric amplification for sub-10-fs pulse generation tunable in the visible and near infrared, Opt. Lett. 23 (16) (1998) 1292–1294.

[27] G. Cerullo, M. Nisoli, S. De Silvestri, Generation of 11 fs pulses tunable across the visible by optical parametric amplification, Appl. Phys. Lett. 71 (25) (1997) 3616–3618.

[28] T. Wilhelm, J. Piel, E. Riedle, Sub-20-fs pulses tunable across the visible from a blue-pumped single-pass noncollinear parametric converter, Opt. Lett. 22 (19) (1997) 1494–1496.

[29] M. Linke, A. Lauer, T. von Haimberger, A. Zacarias, K. Heyne, Three-dimensional orientation of the Q(y) electronic transition dipole moment within the chlorophyll a molecule determined by femtosecond polarization resolved vis pump-IR probe spectroscopy, J. Am. Chem. Soc. 130 (45) (2008) 14904–14905.

[30] G.M. Greetham, P. Burgos, Q. Cao, I.P. Clark, P.S. Codd, R.C. Farrow, M.W. George, M. Kogimtzis, P. Matousek, A.W. Parker, M.R. Pollard, D.A. Robinson, Z.J. Xin, M. Towrie, ULTRA: a unique instrument for time-resolved spectroscopy, Appl. Spectrosc. 64 (12) (2010) 1311–1319.

[31] M. Towrie, D.C. Grills, J. Dyer, J.A. Weinstein, P. Matousek, R. Barton, P.D. Bailey, N. Subramaniam, W.M. Kwok, C. Ma, D. Phillips, A.W. Parker, M.W. George, Development of a broadband picosecond infrared spectrometer and its incorporation into an existing ultrafast time-resolved resonance Raman, UV/visible, and fluorescence spectroscopic apparatus, Appl. Spectrosc. 57 (4) (2003) 367–380.

[32] M. Kaucikas, J. Barber, J.J. Van Thor, Polarization sensitive ultrafast mid-IR pump probe micro-spectrometer with diffraction limited spatial resolution, Opt. Express 21 (7) (2013) 8357–8370.

[33] M.L. Groot, L.J.G.W. van Wilderen, D.S. Larsen, M.A. van der Horst, I.H.M. van Stokkum, K.J. Hellingwerf, R. van Grondelle, Initial steps of signal generation in photoactive yellow protein revealed with femtosecond mid-infrared spectroscopy, Biochemistry 42 (34) (2003) 10054–10059.

[34] K.J. Kubarych, M. Joffre, A. Moore, N. Belabas, D.M. Jonas, Mid-infrared electric field characterization using a visible charge-coupled-device-based spectrometer, Opt. Lett. 30 (10) (2005) 1228–1230.

[35] J. Treuffet, K.J. Kubarych, J.-C. Lambry, E. Pilet, J.-B. Masson, J.-L. Martin, M.H. Vos, M. Joffre, A. Alexandrou, Direct observation of ligand transfer and bond formation in cytochrome c oxidase by using mid-infrared chirped-pulse upconversion, Proc. Natl. Acad. Sci. 104 (40) (2007) 15705–15710.

[36] P. Nuernberger, K.F. Lee, A. Bonvalet, M.H. Vos, M. Joffre, Multiply excited vibration of carbon monoxide in the primary docking site of hemoglobin following photolysis from the heme, J. Phys. Chem. Lett. 1 (14) (2010) 2077–2081.

[37] M.F. DeCamp, L.P. DeFlores, K.C. Jones, A. Tokmakoff, Single-shot two-dimensional infrared spectroscopy, Opt. Express 15 (1) (2007) 233–241.

[38] M.J. Nee, R. McCanne, K.J. Kubarych, M. Joffre, Two-dimensional infrared spectroscopy detected by chirped pulse upconversion, Opt. Lett. 32 (6) (2007) 713–715.

[39] C.R. Baiz, K.J. Kubarych, Ultrabroadband detection of a mid-IR continuum by chirped-pulse upconversion, Opt. Lett. 36 (2) (2011) 187–189.

[40] J.Y. Zhu, T. Mathes, A.D. Stahl, J.T.M. Kennis, M.L. Groot, Ultrafast mid-infrared spectroscopy by chirped pulse upconversion in 1800–1000 cm^{-1} region, Opt. Express 20 (10) (2012) 10562–10571.

[41] P. Hamm, R.A. Kaindl, J. Stenger, Noise suppression in femtosecond mid-infrared light sources, Opt. Lett. 25 (24) (2000) 1798–1800.

[42] R. M.L.V.G. Groot, Femtosecond time-resolved infrared spectroscopy, in: J. T.M. Aartsma (Ed.), Biophysical Techniques in Photosynthesis, Springer, 2008.

[43] P. Hamm, Coherent effects in femtosecond infrared-spectroscopy, Chem. Phys. 200 (3) (1995) 415–429.

[44] M. Joffre, D. Hulin, A. Migus, A. Antonetti, C.B.A. Laguillaume, N. Peyghambarian, M. Lindberg, S.W. Koch, Coherent effects in pump probe spectroscopy of excitons, Opt. Lett. 13 (4) (1988) 276–278.

[45] I.H.M. Van Stokkum, D.S. Larsen, R. Van Grondelle, Global and target analysis of time-resolved spectra, Biochim. Biophys. Acta Bioenerg. 1657 (2004) 82–104.

[46] L.J. van Wilderen, C.N. Lincoln, J.J. van Thor, Modelling multi-pulse population dynamics from ultrafast spectroscopy, PLoS One 6 (3) (2011) e17373.

[47] J.J. Snellenburg, S.P. Laptenok, R. Seger, K.M. Mullen, I.H.M. van Stokkum, Glotaran: a Java-based graphical user interface for the R package TIMP, J. Stat. Softw. 49 (3) (2012) 1–22.

[48] W. Zinth, J. Wachtveitl, The first picoseconds in bacterial photosynthesis — ultrafast electron transfer for the efficient conversion of light energy, ChemPhysChem 6 (5) (2005) 871–880.

[49] M.R. Jones, The petite purple photosynthetic powerpack, Biochem. Soc. Trans. 37 (2009) 400–407.

[50] E. Nabedryk, J.P. Allen, A.K.W. Taguchi, J.C. Williams, N.W. Woodbury, J. Breton, Fourier-transform infrared study of the primary electron-donor in chromatophores of Rhodobacter sphaeroides with reaction centers genetically-modified at residues M160 and L131, Biochemistry 32 (50) (1993) 13879–13885.

[51] E. Nabedryk, J. Breton, J.C. Williams, J.P. Allen, W. Kuhn, W. Lubitz, FTIR character-ization of the primary electron donor in double mutants combining the heterodi-mer HL(M202) with the LH(L131), HF(L168), FH(M197), or LH(M160) mutations, Spectrochim. Acta A Mol. Biomol. Spectrosc. 54 (9) (1998) 1219–1230.

[52] E. Nabedryk, C. Schulz, F. Muh, W. Lubitz, J. Breton, Heterodimeric versus homodi-meric structure of the primary electron donor in *Rhodobacter sphaeroides* reaction centers genetically modified at position M202, Photochem. Photobiol. 71 (5) (2000) 582–588.

[53] E. Nabedryk, S. Andrianambinintsoa, D. Dejonghe, J. Breton, FTIR spectroscopy of the photoreduction of the bacteriopheophytin electron-acceptor in reaction cen-ters of *Rhodobacter sphaeroides* and *Rhodopseudomonas viridis*, Chem. Phys. 194 (2–3) (1995) 371–378.

[54] W.G. Mantele, A.M. Wollenweber, E. Nabedryk, J. Breton, Infrared spectro-electrochemistry of bacteriochlorophylls and bacteriopheophytins — implications for the binding of the pigments in the reaction center from photosynthetic bacteria, Proc. Natl. Acad. Sci. U. S. A. 85 (22) (1988) 8468–8472.

[55] N.P. Pawlowicz, I.H.M. van Stokkum, J. Breton, R. van Grondelle, M.R. Jones, Identi-fication of the intermediate charge-separated state P+beta(−)(L) in a leucine M214 to histidine mutant of the *Rhodobacter sphaeroides* reaction center using femtosecond midinfrared spectroscopy, Biophys. J. 96 (12) (2009) 4956–4965.

[56] J.R. Durrant, G. Hastings, D.M. Joseph, J. Barber, G. Porter, D.R. Klug, Subpicosecond equilibration of excitation-energy in isolated photosystem-II reaction centers, Proc. Natl. Acad. Sci. U. S. A. 89 (23) (1992) 11632–11636.

[57] T. Rech, J.R. Durrant, D.M. Joseph, J. Barber, G. Porter, D.R. Klug, Does slow energy-transfer limit the observed time constant for radical pair formation in photosystem-II reaction centers, Biochemistry 33 (49) (1994) 14768–14774.

[58] D.R. Klug, T. Rech, D.M. Joseph, J. Barber, J.R. Durrant, G. Porter, Primary processes in isolated photosystem-II reaction centers probed by magic-angle transient absorption-spectroscopy, Chem. Phys. 194 (2–3) (1995) 433–442.

[59] S.A.P. Merry, S. Kumazaki, Y. Tachibana, D.M. Joseph, G. Porter, K. Yoshihara, J. Barber, J.R. Durrant, D.R. Klug, Sub-picosecond equilibration of excitation energy in isolated photosystem II reaction centers revisited: time-dependent anisotropy, J. Phys. Chem. 100 (24) (1996) 10469–10478.

[60] M.G. Muller, M. Hucke, M. Reus, A.R. Holzwarth, Primary processes and structure of the photosystem II reaction center. 4. Low-intensity femtosecond transient absorp-tion spectra of D1–D2-cyt-b559 reaction center, J. Phys. Chem. 100 (22) (1996) 9527–9536.

[61] S.R. Greenfield, M. Seibert, Govindjee, M.R. Wasielewski, Wavelength and intensity dependent primary photochemistry of isolated Photosystem II reaction centers at 5 degrees C, Chem. Phys. 210 (1–2) (1996) 279–295.

[62] M.L. Groot, F. Van Mourik, C. Eijckelhoff, I.H.M. Van Stokkum, J.P. Dekker, R. Van Grondelle, Charge separation in the reaction center of photosystem II studied as a function of temperature, Proc. Natl. Acad. Sci. U. S. A. 94 (9) (1997) 4389–4394.

[63] S.R. Greenfield, M. Seibert, Govindjee, M.R. Wasielewski, Direct measurement of the effective rate constant for primary charge separation in isolated photosystem II reaction centers, J. Phys. Chem. B 101 (13) (1997) 2251–2255.

[64] D.R. Klug, J.R. Durrant, J. Barber, The entanglement of excitation energy transfer and electron transfer in the reaction centre of photosystem II, Philos. Trans. R. Soc. Lond. A Math. Phys. Eng. Sci. 356 (1736) (1998) 449–464.

[65] S.R. Greenfield, M. Seibert, M.R. Wasielewski, Time-resolved absorption changes of the pheophytin Q(x) band in isolated photosystem II reaction centers at 7 K: ener-gy transfer and charge separation, J. Phys. Chem. B 103 (39) (1999) 8364–8374.

[66] E. Romero, I.H.M. van Stokkum, V.I. Novoderezhkin, J.P. Dekker, R. van Grondelle, Two different charge separation pathways in photosystem II, Biochemistry 49 (20) (2010) 4300–4307.

[67] J.A. Myers, K.L.M. Lewis, F.D. Fuller, P.F. Tekavec, C.F. Yocum, J.P. Ogilvie, Two-dimensional electronic spectroscopy of the D1-D2-cyt b559 photosystem II reac-tion center complex, J. Phys. Chem. Lett. 1 (19) (2010) 2774–2780.

[68] M.E. Van Brederode, F. Van Mourik, I.H.M. Van Stokkum, M.R. Jones, R. Van Grondelle, Multiple pathways for ultrafast transduction of light energy in the pho-tosynthetic reaction center of *Rhodobacter sphaeroides*, Proc. Natl. Acad. Sci. U. S. A. 96 (5) (1999) 2054–2059.

[69] M.E. Van Brederode, R. Van Grondelle, New and unexpected routes for ultrafast electron transfer in photosynthetic reaction centers, FEBS Lett. 455 (1–2) (1999) 1–7.

[70] M.E. Van Brederode, I.H.M. Van Stokkum, E. Katilius, F. Van Mourik, M.R. Jones, R. Van Grondelle, Primary charge separation routes in the BChl:BPhe heterodimer reaction centers of *Rhodobacter sphaeroides*, Biochemistry 38 (23) (1999) 7545–7555.

[71] B.A. Diner, F. Rappaport, Structure, dynamics, and energetics of the primary photo-chemistry of photosystem II of oxygenic photosynthesis, Annu. Rev. Plant Biol. 53 (2002) 551–580.

[72] L.M.C. Barter, J.R. Durrant, D.R. Klug, A quantitative structure–function relationship for the Photosystem II reaction center: supermolecular behavior in natural photo-synthesis, Proc. Natl. Acad. Sci. U. S. A. 100 (3) (2003) 946–951.

[73] R.N. Frese, M. Germano, F.L. De Weerd, I.H.M. Van Stokkum, A.Y. Shkuropatov, V.A. Shuvalov, H.J. Van Gorkom, R. Van Grondelle, J.P. Dekker, Electric field effects on the chlorophylls, pheophytins, and beta-carotenes in the reaction center of photo-system II, Biochemistry 42 (30) (2003) 9205–9213.

[74] V.I. Prokhorenko, A.R. Holzwarth, Primary processes and structure of the photosys-tem II reaction center: a photon echo study, J. Phys. Chem. B 104 (48) (2000) 11563–11578.

[75] V.I. Novoderezhkin, E. Romero, J.P. Dekker, R. van Grondelle, Multiple charge-separation pathways in photosystem II: modeling of transient absorption kinetics, ChemPhysChem 12 (3) (2011) 681–688.

[76] E. Nabedryk, M. Leonhard, W. Mantele, J. Breton, Fourier-transform infrared differ-ence spectroscopy shows no evidence for an enolization of chlorophyll-a upon

[77] cation formation either invitro or during P700 photooxidation, Biochemistry 29 (13) (1990) 3242–3247.

[77] J. Breton, R. Hienerwadel, E. Nabedryk, in: P. Carmona (Ed.), Spectroscopy of Bio-logical Molecules: Modern Trends, Kluwer, The Netherlands, 1997, p. 101.

[78] T. Noguchi, T. Tomo, Y. Inoue, Fourier transform infrared study of the cation radical of P680 in the photosystem II reaction center: evidence for charge delocalization on the chlorophyll dimer, Biochemistry 37 (39) (1998) 13614–13625.

[79] B.A. Tavitian, E. Nabedryk, W. Mantele, J. Breton, Light-induced Fourier-transform infrared (FTIR) spectroscopic investigations of primary reactions in photosystem-I and photosystem-II, FEBS Lett. 201 (1) (1986) 151–157.

[80] E. Nabedryk, S. Andrianambinintsoa, G. Berger, M. Leonhard, W. Mantele, J. Breton, Characterization of bonding interactions of the intermediary electron-acceptor in the reaction center of photosystem-II by FTIR spectroscopy, Biochim. Biophys. Acta 1016 (1) (1990) 49–54.

[81] T. Noguchi, T. Tomo, C. Kato, Triplet formation on a monomeric chlorophyll in the photosystem II reaction center as studied by time-resolved infrared spectroscopy, Biochemistry 40 (7) (2001) 2176–2185.

[82] B. Loll, J. Kern, W. Saenger, A. Zouni, J. Biesiadka, Towards complete cofactor ar-rangement in the 3.0 angstrom resolution structure of photosystem II, Nature 438 (7070) (2005) 1040–1044.

[83] K.N. Ferreira, T.M. Iverson, K. Maghlaoui, J. Barber, S. Iwata, Architecture of the pho-tosynthetic oxygen-evolving center, Science 303 (5665) (2004) 1831–1838.

[84] A. Zouni, H.T. Witt, J. Kern, P. Fromme, N. Krauss, W. Saenger, P. Orth, Crystal struc-ture of photosystem II from *Synechococcus elongatus* at 3.8 angstrom resolution, Nature 409 (6821) (2001) 739–743.

[85] Z. Liu, H. Yan, K. Wang, T. Kuang, J. Zhang, L. Gui, X. An, W. Chang, Crystal structure of spinach major light-harvesting complex at 2.72 Å resolution, Nature 428 (2004) 287–292.

[86] F.L. de Weerd, M.A. Palacios, E.G. Andrizhiyevskaya, J.P. Dekker, R. van Grondelle, Identifying the lowest electronic states of the chlorophylls in the CP47 core anten-na protein of photosystem II, Biochemistry 41 (51) (2002) 15224–15233.

[87] F.L. de Weerd, I.H.M. van Stokkum, H. van Amerongen, J.P. Dekker, R. van Grondelle, Pathways for energy transfer in the core light-harvesting complexes CP43 and CP47 of photosystem II, Biophys. J. 82 (3) (2002) 1586–1597.

[88] O.A. Sytina, I.H.M. van Stokkum, R. van Grondelle, M.L. Groot, Single and multi-exciton dynamics in aqueous protochlorophyllide aggregates, J. Phys. Chem. A 115 (16) (2011) 3936–3946.

[89] O.A. Sytina, V.I. Novoderezhkin, R. van Grondelle, M.L. Groot, Modeling of multi-exciton transient absorption spectra of protochlorophyllide aggregates in aqueous solution, J. Phys. Chem. A 115 (43) (2011) 11944–11951.

[90] M.A. Palacios, J. Standfuss, M. Vengris, B.F. van Oort, I.H.M. van Stokkum, W. Kühlbrandt, H. van Amerongen, R. van Grondelle, A comparison of the three iso-forms of the light-harvesting complex II using transient absorption and time-resolved fluorescence measurements, Photosynth. Res. 88 (3) (2006) 269–285.

[91] F.J. Kleima, C.C. Gradinaru, F. Calkoen, I.H.M. van Stokkum, R. van Grondelle, H. van Amerongen, Energy transfer in LHCII monomers at 77 K studied by sub-picosecond transient absorption spectroscopy, Biochemistry 36 (49) (1997) 15262–15268.

[92] H.M. Visser, F.J. Kleima, I.H.M. van Stokkum, R. van Grondelle, H. van Amerongen, Probing the many energy-transfer processes in the photosynthetic light-harvesting complex II at 77 K using energy-selective sub-picosecond transient ab-sorption spectroscopy, Chem. Phys. 210 (1–2) (1996) 297–312.

[93] J. Linnanto, J. Martiskainen, V. Lehtovuori, J. Ihalainen, R. Kananavicius, R. Barbato, J. Korppi-Tommola, Excitation energy transfer in the LHC-II trimer: a model based on the new 2.72 Å structure, Photosynth. Res. 87 (3) (2006) 267–279.

[94] T. Bittner, K.-D. Irrgang, G. Renger, M.R. Wasielewski, Ultrafast excitation energy transfer and exciton–exciton annihilation processes in isolated light harvesting complexes of photosystem II (LHC II) from spinach, J. Phys. Chem. 98 (46) (1994) 11821–11826.

[95] H. van Amerongen, R. van Grondelle, Understanding the energy transfer function of LHCII, the major light-harvesting complex of green plants, J. Phys. Chem. B 105 (3) (2000) 604–617.

[96] R. Croce, M.G. Müller, R. Bassi, A.R. Holzwarth, Carotenoid-to-chlorophyll energy transfer in recombinant major light-harvesting complex (LHCII) of higher plants. I. Femtosecond transient absorption measurements, Biophys. J. 80 (2) (2001) 901–915.

[97] J.M. Salverda, M. Vengris, B.P. Krueger, G.D. Scholes, A.R. Czarnoleski, V. Novoderezhkin, H. v. Amerongen, R. v. Grondelle, Energy transfer in light-harvesting complexes LHCII and CP29 of spinach studied with three pulse echo peak shift and transient grating, Biophys. J. 84 (1) (2003) 450–465.

[98] C.C. Gradinaru, I.H.M. van Stokkum, A.A. Pascal, R. van Grondelle, H. van Amerongen, Identifying the pathways of energy transfer between carotenoids and chlorophylls in LHCII and CP29. A multicolor, femtosecond pump–probe study, J. Phys. Chem. B 104 (39) (2000) 9330–9342.

[99] N.E. Holt, J.T.M. Kennis, L. Dall'Osto, R. Bassi, G.R. Fleming, Carotenoid to chlo-rophyll energy transfer in light harvesting complex II from *Arabidopsis thaliana* probed by femtosecond fluorescence upconversion, Chem. Phys. Lett. 379 (3–4) (2003) 305–313.

[100] S.L.S. Kwa, H. van Amerongen, S. Lin, J.P. Dekker, R. van Grondelle, W.S. Struve, Ul-trafast energy transfer in LHC-II trimers from the Chl a/b light-harvesting antenna of Photosystem II, Biochim. Biophys. Acta Bioenerg. 1102 (2) (1992) 202–212.

[101] V.I. Novoderezhkin, M.A. Palacios, H. van Amerongen, R. van Grondelle, Excitation dynamics in the LHCII complex of higher plants: modeling based on the 2.72 Å crystal structure, J. Phys. Chem. B 109 (20) (2005) 10493–10504.

[102] R. van Grondelle, V.I. Novoderezhkin, Energy transfer in photosynthesis: experi-mental insights and quantitative models, Phys. Chem. Chem. Phys. 8 (7) (2006) 793–807.

[103] M.L. Groot, N.P. Pawlowicz, L.J.G.W. van Wilderen, J. Breton, I.H.M. van Stokkum, R. van Grondelle, Initial electron donor and acceptor in isolated Photosystem II reaction centers identified with femtosecond mid-IR spectroscopy, Proc. Natl. Acad. Sci. U. S. A. 102 (37) (2005) 13087–13092.

[104] P. Fromme, P. Jordan, N. Krauß, Structure of photosystem I, Biochim. Biophys. Acta Bioenerg. 1507 (1–3) (2001) 5–31.

[105] P. Jordan, P. Fromme, H.T. Witt, O. Klukas, W. Saenger, N. Krausz, Three-dimensional structure of cyanobacterial photosystem I at 2.5 Angstrom resolution, Nature 411 (6840) (2001) 909–917.

[106] K. Ali, S. Santabarbara, P. Heathcote, M.C.W. Evans, S. Purton, Bidirectional electron transfer in photosystem I: replacement of the symmetry-breaking tryptophan close to the PsaB-bound phylloquinone (A1B) with a glycine residue alters the redox properties of A1B and blocks forward electron transfer at cryogenic temperatures, Biochim. Biophys. Acta Bioenerg. 1757 (12) (2006) 1623–1633.

[107] K. Brettel, W. Leibl, Electron transfer in photosystem I, Biochim. Biophys. Acta Bioenerg. 1507 (1–3) (2001) 100–114.

[108] N. Dashdorj, W. Xu, R.O. Cohen, J.H. Golbeck, S. Savikhin, Asymmetric electron transfer in cyanobacterial Photosystem I: charge separation and secondary electron transfer dynamics of mutations near the primary electron acceptor A0, Biophys. J. 88 (2) (2005) 1238–1249.

[109] W.V. Fairclough, A. Forsyth, M.C.W. Evans, S.E.J. Rigby, S. Purton, P. Heathcote, Bidirectional electron transfer in photosystem I: electron transfer on the PsaA side is not essential for phototrophic growth in Chlamydomonas, Biochim. Biophys. Acta Bioenerg. 1606 (1–3) (2003) 43–55.

[110] M. Guergova-Kuras, B. Boudreaux, A. Joliot, P. Joliot, K. Redding, Evidence for two active branches for electron transfer in photosystem I, PNAS 98 (8) (2001) 4437–4442.

[111] N. Ivashin, S. Larsson, Electron transfer pathways in photosystem I reaction centers, Chem. Phys. Lett. 375 (3–4) (2003) 383–387.

[112] O.G. Poluektov, S.V. Paschenko, L.M. Utschig, K.V. Lakshmi, M.C. Thurnauer, Bidirectional electron transfer in photosystem I: direct evidence from high-frequency time-resolved EPR spectroscopy, J. Am. Chem. Soc. 127 (34) (2005) 11910–11911.

[113] W. Xu, P.R. Chitnis, A. Valieva, A. van der Est, K. Brettel, M. Guergova-Kuras, Y.N. Pushkar, S.G. Zech, D. Stehlik, G. Shen, B. Zybailov, J.H. Golbeck, Electron transfer in cyanobacterial photosystem I: II. Determination of forward electron transfer rates of site-directed mutants in a putative electron transfer pathway from A0 through A1 to FX, J. Biol. Chem. 278 (30) (2003) 27876–27887.

[114] M.G. Müller, C. Slavov, R. Luthra, K.E. Redding, A.R. Holzwarth, Independent initiation of primary electron transfer in the two branches of the photosystem I reaction center, PNAS 107 (9) (2010) 4123–4128.

[115] W. Giera, V.M. Ramesh, A.N. Webber, I. van Stokkum, R. van Grondelle, K. Gibasiewicz, Effect of the P700 pre-oxidation and point mutations near A0 on the reversibility of the primary charge separation in Photosystem I from Chlamydomonas reinhardtii, Biochim. Biophys. Acta Bioenerg. 1797 (1) (2010) 106–112.

[116] A.R. Holzwarth, M.G. Müller, J. Niklas, W. Lubitz, Ultrafast transient absorption studies on photosystem I reaction centers from Chlamydomonas reinhardtii. 2: mutations near the P700 reaction center chlorophylls provide new insight into the nature of the primary electron donor, Biophys. J. 90 (2) (2006) 552–565.

[117] J. Breton, Fourier transform infrared spectroscopy of primary electron donors in type I photosynthetic reaction centers, Biochim. Biophys. Acta Bioenerg. 1507 (1–3) (2001) 180–193.

[118] J.-R. Burie, A. Boussac, C. Boullais, G. Berger, T. Mattioli, C. Mioskowski, E. Nabedryk, J. Breton, FTIR spectroscopy of UV-generated quinone radicals: evidence for an intramolecular hydrogen atom transfer in ubiquinone, naphthoquinone, and plastoquinone, J. Phys. Chem. 99 (12) (1995) 4059–4070.

[119] G. Hastings, K.M.P. Bandaranayake, E. Carrion, Time-resolved FTIR difference spectroscopy in combination with specific isotope labeling for the study of A(1), the secondary electron acceptor in photosystem 1, Biophys. J. 94 (11) (2008) 4383–4392.

[120] V. Sivakumar, R. Wang, G. Hastings, A1 reduction in intact cyanobacterial photosystem I particles studied by time-resolved step-scan Fourier transform infrared difference spectroscopy and isotope labeling, Biochemistry 44 (6) (2005) 1880–1893.

[121] T. Renger, E. Schlodder, Primary Photophysical Processes in Photosystem II: Bridging the Gap between Crystal Structure and Optical Spectra, Chemphyschem. 11 (6) (2010) 1141–1153.

[122] A.D. Stahl, M. Di Donato, I.H.M. van Stokkum, R. van Grondelle, M.L. Groot, Closed reaction centers of PS1 still can perform the first steps of charge separation. A mid IR pump probe study with fs resolution, in: T. Kuang, C. Lu, L. Zhang (Eds.), Photosynthesis Research for Food, Fuel and the Future, Springer, Berlin Hidelberg, 2013, pp. 127–130.

[123] N.K. Preketes, J.D. Biggs, H. Ren, I. Andricioaei, S. Mukamel, Simulations of two-dimensional infrared and stimulated resonance Raman spectra of photoactive yellow protein, Chem. Phys. 422 (2013) 63–72.

[124] F. Xia, T. Rudack, C. Kotting, J. Schlitter, K. Gerwert, The specific vibrational modes of GTP in solution and bound to Ras: a detailed theoretical analysis by QM/MM simulations, Phys. Chem. Chem. Phys. 13 (48) (2011) 21451–21460.